

RESEARCHES UPON THE CAVITATION PHENOMENON OF THE CENTRIFUGAL PUMPS

Beazit ALI¹

Anastase PRUIU²

Levent ALI³

Ion Adrian GIRBA⁴

¹Professor, PhD. Eng., "Mircea cel Batran" Naval Academy, Constanta

²Professor, PhD. Eng., "Mircea cel Batran" Naval Academy, Constanta

³Eng. PhD attendee Military Technical Academy, Bucharest

⁴Eng. PhD attendee Military Technical Academy, Bucharest

Abstract: The main problem of the hydrodynamics of cavitation implosion of a single bubble, consists in pressure and velocity fields determination, including the collapse velocity of the bubble wall. The bubble surface is a discontinuity surface, and the overpressure produced by a bubble collapse are very great (many thousands bar) facts that suggests the opportunity of the distribution theory use. We use from in distribution of the equations for a non viscous, incompressible liquid. Using the Dirac filtering property some integral equations were obtained, giving the liquid velocity and pressure fields due to the bubble's implosion. By analysis the theoretic and experimental phenomenon it establish the implicit function which describes this phenomenon. By application the Π theorem for this implicit function it finds the criterion equation of phenomenon. Depending on operating condition various cavitation patterns can be observed on a body surface as travelling bubbles, attached sheet cavitation, shear cavitation or vortex cavitation. Leading edge attached partial cavitation is commonly encountered on rotor blades or on hydrofoil. It corresponds to the case for which a vapor cavity is attached in the vicinity of the leading edge and extends over a fraction of the foil surface. It generally takes places at incidence angles for which a leading edge pressure peak occurs and reduced below the liquid vapor pressure. At the early phases of development, leading edge partial cavitation is steady.

INTRODUCTION

The main problem of the hydrodynamics of cavitation implosion of a single bubble, consists in pressure and velocity fields determination, including the collapse velocity of the bubble wall. The bubble surface is a discontinuity surface, and the overpressure produced by a bubble collapse are very great (many thousands bar) facts that suggests the opportunity of the distribution theory use.

THEORETICAL PROBLEMS

Let's write the equations of the mechanics of the light fluid at distribution.

It is considered a closed surface $S(\bar{r}, t) = 0$ which delimits an internal domain D_i from an external domain D_e , unlimited, filled with fluid.

The local form of the continuity equation, valid in the absence of the discontinuous surfaces, is:

$$\frac{\partial \rho}{\partial t} + \text{div}(\rho \bar{v}) = 0 \quad (1)$$

we choose $\theta(\bar{r}, t)$ to be the characteristic function

of the D^i domain defined by:

$$\theta(\bar{r}, t) = \theta(x, y, z, t) = \begin{cases} 1 & \text{for } (x, y, z) \in D \\ 0 & \text{for } (x, y, z) \notin D \end{cases} \quad (2)$$

we obtain:

$$\rho = \rho^{(i)}\theta + \rho^{(e)}(1 - \theta) \quad (3)$$

$$\bar{v} = \bar{v}^{(i)}\theta + \bar{v}^{(e)}(1 - \theta)$$

assuming that all the functions are $C^2(D^i)$ and $C^2(D^e)$. We use the formula:

$$\frac{\partial \theta(\bar{r}, t)}{\partial t} = (\bar{d} \cdot \bar{n}) \delta_s \quad (4)$$

$$\text{grad} \theta(\bar{r}, t) = -\bar{n} \delta_s \quad (5)$$

where \bar{d} represents the local velocity of the mobile surface $S(\bar{r}, t) = 0$ and δ_s is the Dirac distribution associated with this surface.

By introducing (2) and (3) in (1) and using (4) and (5) according to the vectorial analysis calculations we obtain:

$$0 = \frac{\partial \rho}{\partial t} + \text{div}(\rho \bar{v}) = \left\{ \frac{\partial \rho^{(i)}}{\partial t} + \text{div}(\rho^{(i)} \bar{v}^{(i)}) \right\} \theta + \left\{ \frac{\partial \rho^{(e)}}{\partial t} + \text{div}(\rho^{(e)} \bar{v}^{(e)}) \right\} (1 - \theta) + [\rho(\bar{v} - \bar{d}) \cdot \bar{n}]_s$$

Due to the fact that for each of the domains D_i and D_e , the continuity equation remains valid, the formulas between brackets are null. Consequently, in distributions, the form of the continuity equation is valid anywhere $D^i \cup S(\bar{r}, t) \cup D^e$ and it is:

$$\frac{\partial \rho}{\partial t} + \text{div}(\rho \bar{v}) = [\bar{\rho}(\bar{v} - \bar{d})\bar{n}]_s \delta_s \quad (6)$$

Analogously (4), the Euler equation in the formula stated by Helmholtz, valid in the absence of the discontinuous surfaces has the following formula:

$$\frac{\partial \bar{v}}{\partial t} + \text{grad} \frac{(\bar{v})^2}{2} - \bar{v} \text{rot} \bar{v} = \bar{f}^{(m)} - \frac{1}{\rho} \text{grad} p \quad (7)$$

and in the presence of the discontinuous surface S:

$$\begin{aligned} \frac{\partial \bar{v}}{\partial t} + \text{grad} \frac{(\bar{v})^2}{2} - \bar{v} \text{rot} \bar{v} = \\ = \bar{f}^{(m)} - \frac{1}{\rho} \text{grad} p + [\bar{\rho}(\bar{v} - \bar{d})\bar{n}]_s \delta_s + [p]_s \bar{n} \delta_s \end{aligned}$$

valid in $D^i \cup S \cup D^e$, where $\bar{f}^{(m)}$ represents the field of the massic forces and $[p]_s$ is the pressure scale which separates the two domains.

Observation: it is known from (1) that the effect of the viscosity in the cavitation phenomenon is very low, that is when considering the Euler equations, valid for the ideal fluids (light), is legitimate.

Hypothesis

It is considered an unlimited, incompressible, light fluid in which there is a spherical cavitation bubble, with the initial radius R_0 , empty on the inside. The fluid movement of the implosion of the bubble is considered irrational $\text{rot} \bar{v}(\bar{r}, t) = 0$ and the massic forces field is unvalued $\bar{f}^{(m)} = 0$.

Using the spherical coordinates, originated in the centre of the bubble, symmetrically, is enough for the study of the radial direction, reducing to a one-dimensional problem.

The closed surface $S(\bar{r}, t) = 0$ is assimilated by a sphere with the equation $r = R(t)$, the local velocity of the surface becomes $\dot{R}(t)$, representing the implosion velocity of the bubble wall.

The mathematic pattern

In the spherical coordinates, the Dirac distribution (4) associated with the surface $S(\bar{r}, t) = 0$ ($r = R(t)$) is:

$$\delta_{S(r,t)} = \frac{\delta(r - R(t))}{4\pi R^2(t)}$$

In addition, in the spherical coordinates, the form of the vectorial differential operators which intervene in equation (6) and (7) is used:

$$\frac{\partial \rho}{\partial t} + \frac{1}{r^2} \frac{\partial}{\partial r} (r^2 \rho v(r, t)) = \rho [v(r, t) - \dot{R}(t)] \quad (8)$$

$$\frac{\delta(r - R(t))}{4\pi R^2(t)}$$

$$\frac{\partial v}{\partial t} + v \frac{\partial v}{\partial r} + \frac{1}{\rho} \frac{\partial p}{\partial r} [\rho v(r, t) - \dot{R}(t)] = \quad (9)$$

$$\frac{\delta(r - R(t))}{4\pi R^2(t)} + [p]_s \frac{\delta(r - R(t))}{4\pi R^2(t)}$$

$$\lim_{r \rightarrow +\infty} p(r, t) = p_\infty \quad \text{where } p_\infty \text{ is a constant}$$

$$\lim_{r \rightarrow +\infty} v(r, t) = 0,$$

$$\rho(r, t) = \rho_e \cdot H_{R(t)}(r) = \begin{cases} \rho_e & \text{pentru } r \geq R(t) \\ 0 & \text{pentru } 0 < r < R(t) \end{cases}$$

ρ_e is for the density of the fluid, $H_{R(t)}(r)$ is Haviside's unit step function of the $R(r)$ parameter.

$$\text{Observation: } \frac{\partial \rho}{\partial t} = 0$$

The implosion velocity of the bubble $r = R(t)$ is given by Rayleigh's classic formula (non-linear differential equation) obtained in (2) especially using the kinetic energy theorem:

$$R(t) = \sqrt{\frac{2}{3} \frac{p_\infty}{\rho_e} \left[\left(\frac{R_0}{R(t)} \right)^3 - 1 \right]} \quad (10)$$

where $R_0 = R(t)_{t=0}$.

Calculus

The difficulties derive from the fact that: the system of differential equations with partial derivatives is non-linear and the distribution in the spherical coordinates depends on several parameters.

The only advantage is that the equations are linked, that is from (8) may result $v(r, t)$ and then, knowing $v(r, t)$, from (9) may result $\rho(r, t)$.

In order to apply the filtration property of the Dirac distribution:

$$\int_{-\infty}^{+\infty} f(x) \delta(x - x_0) dx = f_{x_0}$$

under:

$$\int_{-\infty}^{+\infty} f(r, t) \delta(r - R(t)) dr = f(R(t), t)$$

in the equations (8) and (9) we artificially extend the definition domain of the functions

$p(r, t)$ and $v(r, t)$:

$$\tilde{p}(r, t) = \begin{cases} p(r, t) & \text{pentru } r \geq 0 \text{ si } t \geq 0 \\ 0 & \text{pentru } r < 0 \text{ si } t < 0 \end{cases}$$

analogously for $v(r, t)$.

Equation(8) becomes:

$$\begin{aligned} \int_{-\infty}^{+\infty} \frac{1}{r^2} \frac{\partial}{\partial r} (r^2 \rho(r, t) \tilde{v}(r, t)) dr = \\ = \int_{-\infty}^{+\infty} \frac{\tilde{\rho}(r, t)}{4\pi R^2(t)} [\tilde{v}(r, t) - \dot{R}(t)] \rho(r - R(t)) dr \end{aligned} \quad (8')$$

For the left part of the equation (8') several calculi are necessary:

$$\frac{1}{r^2} \frac{\partial}{\partial r} (r^2 v(r, t)) = \frac{1}{r^2} r^2 \frac{\partial}{\partial r} (v(r, t)) - \frac{1}{r^2} 2rv(r, t)$$

because the density is 0 for $r < R(t)$, the inferior integration limit is $R(t)$ not $-\infty$ using the asymptomatic condition $\lim_{r \rightarrow +\infty} v(r, t) = 0$

$$\int_{R(t)}^{+\infty} \frac{\partial}{\partial r} \tilde{v}(r, t) dr = \tilde{v}(r, t) \Big|_{R(t)}^{+\infty} = 0 - v(R(t), t)$$

The equation (8') becomes:

$$\rho e \left[-\tilde{v}(R(t), t) + 2 \int_{R(t)}^{+\infty} \frac{v(r, t)}{r} dr \right] = \quad (11)$$

$$= \frac{\rho(R(t), t)}{4\pi R^2(t)} [\tilde{v}(r(t), t) - \dot{R}(t)]$$

but for $r \geq R(t)$
$$\begin{cases} \tilde{v}(r, t) = v(r, t) \\ \rho(R(t), t) = \rho e \\ v(R(t), t) = \dot{R}(t) \end{cases}$$

it results:
$$\int_{R(t)}^{+\infty} \frac{v(r, t)}{r} dr = \frac{1}{2} \dot{R}(t)$$

where $\dot{R}(t)$ and $R(t)$ are known from (10).

It can be observed that the integral depends only on the velocity values at the bubble wall. By applying the same treatment as before to the equation (9), we obtain:

$$\int_{R(t)}^{+\infty} \frac{\partial}{\partial t} \left(v + \frac{v^2}{2} \right) dr + \frac{1}{\rho e} \int_{R(t)}^{+\infty} \frac{\partial p}{\partial r} dr =$$

$$= \rho e [v(R(t), t)(v(R(t), t) - \dot{R}(t))] \cdot \frac{1}{4\pi R^2(t)} + \frac{p(R(t), t)}{4\pi R^2(t)}$$

because $v(R(t), t) = \dot{R}(t)$ the first formula of the right element is null.

$$\int_{R(t)}^{+\infty} \frac{\partial p}{\partial r} dr = p_{\infty} - p(R(t), t) \quad (12)$$

$$\int_{R(t)}^{+\infty} \frac{\partial}{\partial t} \left(v + \frac{v^2}{2} \right) dr + \frac{p_{\infty}}{\rho e} = p(R(t), t) \cdot \left[\frac{1}{4\pi R^2(t)} + \frac{1}{\rho e} \right]$$

USING THE SIMILITUDE THEORY ON TWO SCALES IN THE EXPERIMENTAL STUDY OF THE CAVITATION PHENOMENON

There are situations when the possibilities of accomplishment of the pattern impose exceptions from the complete geometrical similitude, obtaining this way the distorted patterns which have horizontal lengths and vertical lengths reduced to different scales.

Generally, the distorted patterns are imposed when the possibilities of practical accomplishment make impossible the exact conformation of the geometrical similitude between the pattern and the prototype, or when evolution of the phenomenon on the pattern made at a single scale would lead to a laminar movement instead of turbulent one which would make all the experiments difficult.

A random physical phenomenon can be expressed in the most general way through a function of several physical proportions and the establishment of the connection between them is

made (when the number of the physical proportions $n \geq 5$) through theorem II.

Any homogeneous function of several physical proportions which determine a physical phenomenon can always be reduced to a relation between dimensionless complex proportions of the following formula:

$$\Phi(\Pi_1, \Pi_2, \dots, \Pi_{n-k}) = 0$$

In the theory of similitude this function is called criteria equation and its establishment represents the first phase of the pattern study of a phenomenon.

As it is known the cavitation problems have not yet been solved, theoretically or practically, worldwide, although researches are made to this respect.

If we want to study this phenomenon through the similitude theory, we should previously set the physical proportions that intervene within the evolution of the cavitation phenomenon on the rotor of the axial pumps.

The criteria equation for the cavitation phenomenon produced at the wheels of the axial pumps

After theoretical and experimental researches made until now, it has been established that the cavitation phenomenon at the rotor of the axial pumps has the following implicit function:

$$f(\rho, n, D, T, \Delta p, h, d_{\max}, g, \eta, v, m, z) = 0 \quad (13)$$

where:

ρ - water density

n - wheel speed

D - wheel diameter

T - wheel pusher

$\Delta p = p - p_v$ - pressure distribution on the blade

p_v - water vaporization pressure at certain temperature;

h - immersion of the wheel axis on the water surface

d_{\max} - maximum thickness of the wheel blade;

g - gravitational velocity $g = 9,81 \text{ m/s}^2$;

η - water kinetic viscosity ;

v - current velocity through the rotor disk;

m - air volume dissolved in water;

z - number of the wheel blades.

The physical proportions of this implicit function actually represent the physical proportions which this phenomenon depends on.

In order to apply theorem II to the implicit function, we first write the dimensional matrix of the variables (number of rotor blades z is the same both as pattern and prototype).

$$\begin{array}{cccccccccccc} \rho & n & D & T & \Delta p & h & d_{\max} & g & \eta & v & m \\ m & -3 & 0 & 1 & 1 & -1 & 1 & 1 & -1 & 1 & 0 \\ Kg & 1 & 0 & 0 & 1 & 1 & 0 & 0 & 0 & 1 & 0 & 1 \\ s & 0 & -1 & 0 & -2 & -2 & 0 & 0 & -2 & -1 & -1 & 0 \end{array} \quad (14)$$

$$\begin{pmatrix} -3 & 0 & 1 & 1 & -1 & 1 & 1 & 1 & -1 & 1 & 0 \\ 1 & 0 & 0 & 1 & 1 & 0 & 0 & 0 & 1 & 0 & 1 \\ 0 & -1 & 0 & -2 & -2 & 0 & 0 & -2 & -1 & -1 & 0 \end{pmatrix}$$

out of which we obtain the equations system:

$$\begin{cases} -3x_1 + x_3 + x_4 - x_5 + x_6 + x_7 + x_8 - x_9 + x_{10} = 0 \\ x_1 + x_4 + x_5 + x_9 + x_{11} = 0 \\ -x_2 - 2x_4 - 2x_5 - 2x_8 - x_9 - x_{10} = 0 \end{cases} \quad (15)$$

We sort out the main variables of the system:

$$\begin{aligned} x_1 &= -x_4 - x_5 - x_9 - x_{11} \\ x_2 &= -2x_4 - 2x_5 - 2x_8 - x_9 - x_{10} \\ x_3 &= -4x_4 - 2x_5 - x_6 - x_7 - x_8 - 2x_9 - x_{10} - 3x_{11} \end{aligned} \quad (16)$$

System (3) is undetermined for solving, so we apply the Cramer rule and we obtain the solution matrix as it follows:

$$\begin{array}{cccccccccccc} \rho & n & D & T & \Delta p & h & d_{\max} & g & \eta & v & m \\ \Pi_1 & -1 & -2 & -4 & 1 & 0 & 0 & 0 & 0 & 0 & 0 \\ \Pi_2 & -1 & -2 & -2 & 0 & 1 & 0 & 0 & 0 & 0 & 0 \\ \Pi_3 & 0 & 0 & -1 & 0 & 0 & 1 & 0 & 0 & 0 & 0 \\ \Pi_4 & 0 & 0 & -1 & 0 & 0 & 0 & 1 & 0 & 0 & 0 \\ \Pi_5 & 0 & -2 & -1 & 0 & 0 & 0 & 0 & 1 & 0 & 0 \\ \Pi_6 & -1 & -1 & -2 & 0 & 0 & 0 & 0 & 0 & 1 & 0 \\ \Pi_7 & 0 & -1 & -1 & 0 & 0 & 0 & 0 & 0 & 0 & 1 \\ \Pi_8 & -1 & 0 & -3 & 0 & 0 & 0 & 0 & 0 & 0 & 1 \end{array} \quad (17)$$

Out of the solution matrix we obtain the following similitude criteria:

$$\begin{aligned} \Pi_1 &= \frac{T}{\rho n^2 D^4}; \Pi_2 = \frac{p - p_v}{\rho n^2 D^2}; \Pi_3 = \frac{h}{D}; \Pi_4 = \frac{d_{\max}}{D}; \\ \Pi_5 &= \frac{g}{n^2 D}; \Pi_6 = \frac{\eta}{\rho n D^2}; \Pi_7 = \frac{v}{n D}; \Pi_8 = \frac{m}{\rho D^3} \end{aligned} \quad (18)$$

The criteria equation in which we shall include the number of blades z , shall be as it follows:

$$\varphi\left(\frac{T}{\rho n^2 D^4}, \frac{p - p_v}{\rho n^2 D^2}, \frac{h}{D}, \frac{d_{\max}}{D}, \frac{g}{n^2 D}, \frac{\eta}{\rho n D^2}, \frac{v}{n D}, \frac{m}{\rho D^3}, z\right) = 0 \quad (19)$$

If we respect the geometrical similitude after a single scale, it is possible that the thickness of the wheel blade and the immersion of its axis to reduce a lot, therefore it is possible that the pattern not to be able to be used for determinations, the results including too many errors.

Because of this, it is more advantageous and safe to create the distorted blade pater (at two scales), which allows more accurate results.

It can be determined the pattern law in the case of similitude at two scales, by randomly choosing the scale of the parallel lengths with the blade diameter and the scale of the parallel lengths with the thickness of the blade.

EXPERIMENTAL RESULTS AND DISCUSSIONS

An investigation of leading edge partial cavitation was performed in Romania (ICEPRONAV – Galați) including the conditions of cavitation inception, the cavitation patterns together with cavity length measurements. The investigation was enhanced by instantaneous wall-pressure measurements using an instrumented blade of rotor equipped with seventeen wall-pressure transducers mounted into small cavities, (fig 1).

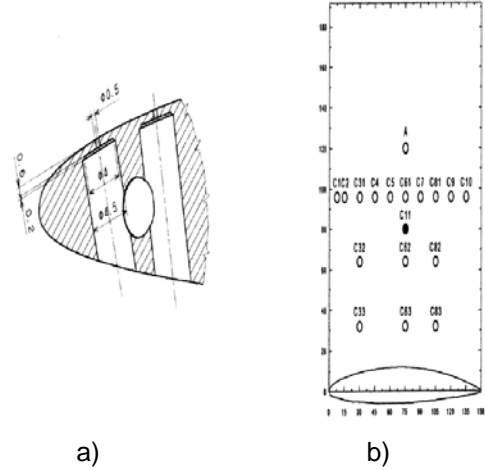


Fig. 1, a) Transducer cavity, b) Location of the pressure transducers, filled symbol is on the pressure side, A referees to an accelerometer, unit in millimeter

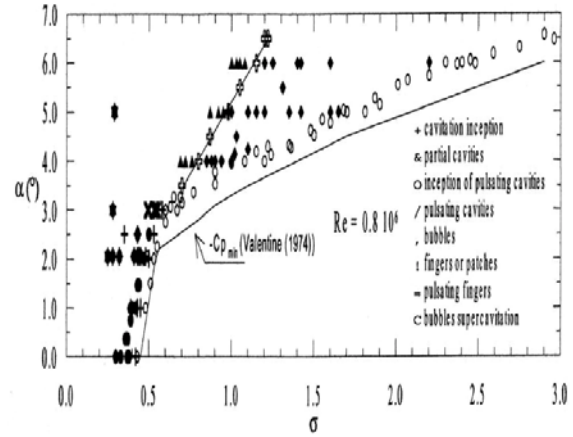


Fig. 2

All the experiments fitted with a 1m long and 0,192 m wide square cross test section. In this device, velocities of up to 15 m/s and pressures between 30 mbar and 3 bar can achieved. The designed blade for this project is a 0,191 mm span two - dimensional cambered foil of the NACA 66 . Several experimental results have been obtained. Figure 2 shows the inception conditions and the various patterns detected on the suction side of the foil versus the cavitation number and the angle of incidence. The inception conditions are also compared to the theoretical values of the opposite of the minimum pressure

coefficient on the suction side. Partial cavities of intermediate length (l^* lower than about 0,5) have a relatively stable behavior with weak variation of the cavity closure while shedding U-shaped vapor structures in the wake. In that situation the cavity length was measurable (see fig. 3). As shown on fig. 4, the liquid-vapor interface has a glossy aspect over a short distance from the leading edge indicative of a laminar boundary layer developing on the interface. The extent of the laminar flow was found to be dependent on the velocity (Figures 4.b and 4.c for the same cavitation number but two velocities). Further away the interface becomes wavy and unstable over a large fraction of the cavity length. When the cavity becomes large, typically l/c larger than about 0,5, it exhibits a pulsating behavior while shedding larger vapor-filled structures. The transition is relatively well represented by the straight line shown on fig 1.

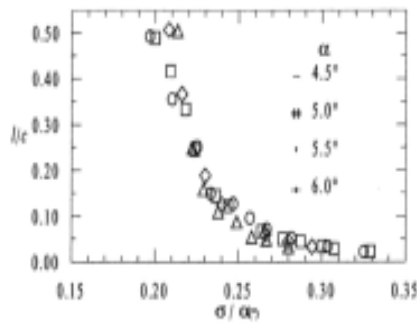


Fig. 3 Cavity length as a function of $\frac{\sigma}{\alpha}$,
 $Re = 8 \cdot 10^6$

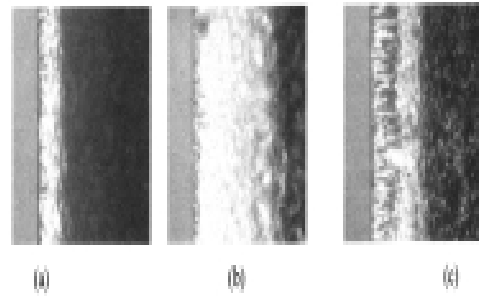


Fig. 4. Photographs of leading edge partial sheet cavitation, NACA 66-12% - 100mm foil, flow is from the left, $\alpha = 6$, a) $Re = 8 \cdot 10^6$, $\sigma = 1,98$, $l/c = 0,045$ b) $Re = 8 \cdot 10^6$, $\sigma = 1,31$, $l/c = 0,325$. c) $Re = 0,4 \cdot 10^6$, $\sigma = 1,30$, $l/c = 0,205$.

CONCLUSIONS

Used in distributions, the equations form in the fluid mechanics and the filtration property of the Dirac distribution, several integral formulas regarding the cavitation implosion are obtained.

The mathematic pattern, which only describes the fluid movement, can only indicate something about the hydrodynamic effects of the cavitation implosion, the thermal and electrochemical effects, experimentally presented, can be analogously analyzed.

After knowing the non dimensional complex numbers which form the criteria equation, before making the pattern of the studied phenomenon we shall establish the connections between the scales of the physical proportions which determine these complex numbers, that is we shall establish the pattern law.

Being familiar to the distorted pattern law, we can transfer the proportions results obtained on the pattern, on the prototype.

We notice that not all the similitude criteria have the same importance in the evolution of the cavitation process of the axial pumps blades. The most important criterion, decisive in the cavitation process, is the one in which the vaporization pressure intervenes p_v .

The cavity length does not change significantly, the liquid – vapor interface is smooth and has a glossy aspect along a short distance from the leading edge. At the end of the cavity it breaks partially into small bubbles. As the cavity expands, the liquid – vapor interface become distorted, wavy and unstable yielding to breakup and unsteadiness. At this stage significant variations of the location of the cavity closure point are observed while shedding vapor structures called „cloud” cavitation. This process induces high - level pressure pulses and is known to be one of the most destructive forms of cavitation.

BIBLIOGRAPHY:

- [1] I. Anton, *Cavitation*, Bucharest, 1984
- [2] G. Baran, *Cavitation*, Course of the Polytechnic Institute Bucharest, 1994
- [3] L. Burlacu, *Analytical Mathematics*, Bucharest, 1983
- [4] C. Iacob, *Classical and modern mathematics*, vol. IV, Bucharest, 1984
- [5] I. Anton, *Cavitation*, vol. I and II, Academy Publishing, Bucharest, 1980
- [6] B. Ali, *Hydrodynamics of the wing span, control of cavitation and the stability of the hydrofoil ship*, Scientific Paper II, Galati, 1996
- [7] Al. A. Vasilescu, *Dimensional analysis and the similitude theory*, Academy Publishing, Bucharest, 1969.
- [8] V. Teodorescu, *Equations of mathematical physics*, Course of the University of Bucharest, 1982.